On the internal rotations in *p*-cresol in its ground and first electronically excited states

Arnim Hellweg and Christof Hättig
Lehrstuhl für Theoretische Chemie, Ruhr-Universität Bochum, D-44780 Bochum, Germany

(Received 4 April 2007; accepted 1 June 2007; published online 12 July 2007)

The overall rotation and internal rotation of *p*-cresol (4-methyl-phenol) has been studied by comparison of the microwave spectrum with accurate *ab initio* calculations using the principal axis method in the electronic ground state. Both internal rotations, the torsions of the methyl and the hydroxyl groups relative to the aromatic ring, have been investigated. The internal rotation of the hydroxyl group can be approximately described as the motion of a symmetrical rotor on an asymmetric frame. For the methyl group it has been found that the potential barrier hindering its internal rotation is very small with the first two nonvanishing Fourier coefficients of the potential V_3 and V_6 in the same order of magnitude. Different splittings of *b*-type transitions for the *A* and *E* species of the methyl torsion indicate a top-top interaction between both internal rotors through the benzene ring. An effective coupling potential for the top-top interaction could be estimated. The hindering barriers of the hydroxyl and methyl rotation have been calculated using second-order Møller-Plesset perturbation theory and the approximate coupled-cluster singles-and-doubles model (CC2) in the ground state and using CC2 and the algebraic diagrammatic construction through second order in the first electronically excited state. The results are in excellent agreement with the experimental values. © *2007 American Institute of Physics*. [DOI: 10.1063/1.2752163]

I. INTRODUCTION

Studies of internal rotations have a long history of experimental and computational studies.[1–5] Rotational resolved spectroscopy in the gas phase is suitable to obtain very accurate values for the potential barriers hindering the internal motions, and investigations in the electronic ground state are performed since over 50 years.[6,7] In the last two decades experimental setups are also available, which allow the investigation of internal motions in electronically excited states.[8]

The theoretical description of these motions, particularly in the excited states, is a demanding test for *ab initio* methods. Although a decent qualitative description of internal rotations can often be achieved at the Hartree-Fock level, a quantitative analysis requires an accurate accounting for of electron correlation effects.[9] Recently, accurate *ab initio* methods for calculations on electronically excited states, which include electron correlation with reasonable computational costs, have become available.[10]

The present publication concludes a series of combined microwave and quantum chemical studies on cresols.[11,12] *p*-cresol is currently under investigation in very different fields of chemistry: In atmospheric chemistry as a precursor for the formation of photo-oxidants and secondary organic aerosols,[13] in clinical chemistry for its influence on kidney failures,[14] and in food chemistry where *p*-cresol has been spotted to have an influence on the composition of the aroma of cheddar cheese.[15]

For *para* substituted toluenes with a C_6 symmetry of the internal rotor (toluene,[16] *p*-fluorotoluene,[17] and *p*-chlorotoluene[18]), very low barriers hindering the methyl torsion of less than 5 cm^{-1} were found. In *p*-cresol the potential for the internal rotation of the methyl group is also almost C_6 symmetric, only distorted by the interaction with the hydroxyl group in *para* position to C_3 symmetry. One of the questions that had to be solved for the present study has been how such a rotation is described best for a theoretical analysis. Another objective has been the study of the internal rotation of the hydroxyl group. This internal motion could not be investigated in the previous studies on *o*- and *m*-cresol[11,12] because in these cases it leads to a tilt of the molecular principal axis system and thus to two distinct conformers. The theoretical background of hindered rotations in C_2 symmetric potentials has been derived by Quade[19] and Bauder *et al.*[20] The methods were employed, e.g., for phenol,[21] 4-fluorophenol, 4-chlorophenol, and 4-bromophenol.[22]

Theoretical investigations of *p*-cresol go back to Kudchadker *et al.*,[23] where the conformational energy differences for the methyl group and the hydroxyl group were analyzed with the semiempirical complete neglect of differential overlap/2 method. Hameka and Jensen[24] reported geometries, vibrational frequencies, and excitation energies of toluene and *p*-cresol from four in four complete active space self-consistent field (SCF) computations with a 6-31G basis set. A qualitative description of the S_0-S_1 excitation is given, although no accurate quantitative results could be determined. The absorption bands were overestimated by far. Richardson *et al.*[25] investigated alkyl and hydroxyl rotations in *p*-alkyl phenols (including *p*-cresol) theoretically at the MP2/6-31G(*d*,*p*) level in S_0. Ring mediated interactions of these internal rotations were found.

Experimentally, the internal rotations in *p*-cresol and its water clusters have been investigated by Schmitt[26] in S_0 and

 © 2007 American Institute of Physics

Downloaded 23 Aug 2008 to 134.147.252.238. Redistribution subject to AIP license or copyright; see http://jcp.aip.org/jcp/copyright.jsp

S_1 and later in the same group by Myszkiewicz *et al.*[27] with rotationally resolved laser-induced fluorescence spectroscopy in the S_1 state. Accurate molecular parameters for the excited state could be obtained thereby.

In the present work we report an investigation of the internal rotations of *p*-cresol in its electronic ground state with the second-order Møller-Plesset perturbation theory (MP2) and the approximate coupled-cluster singles-and-doubles model[28] (CC2). The theoretical results are compared with very accurate data from pulsed nozzle molecular beam Fourier-transform microwave spectroscopy. For the theoretical investigation of the first electronically excited state CC2 and the algebraic diagrammatic construction through second order[29,30] [ADC(2)] have been employed. High-level basis sets have been used throughout to minimize the basis set incompleteness error and to take full advantage of the accuracy of these methods.

II. OVERALL AND INTERNAL ROTATION

The Hamiltonian of a molecular rotation with a symmetrical internal rotor can be written as a sum of different contributions.[6,7]

$$\hat{H} = \hat{H}_{\mathrm{rot}} + \hat{H}_{\mathrm{cd}} + \hat{H}_{\mathrm{ir}}. \tag{1}$$

The pure overall-rotational part is equivalent to an asymmetric top in classical mechanics and can conveniently be expressed as a rotation around the principal axis.

$$\hat{H}_{\mathrm{rot}} = A\hat{J}_a^2 + B\hat{J}_b^2 + C\hat{J}_c^2. \tag{2}$$

In the centrifugal distortion part we only needed to include terms up to fourth order in the components $\hat{J}_g$, $g \in \{a,b,c\}$, of the angular momentum operator $\hat{J}$ using Watson's *S* reduction[31] in the I^r representation

$$\hat{H}_{\mathrm{cd}} = -D_J\hat{J}^4 - D_{JK}\hat{J}^2\hat{J}_a^2 - D_K\hat{J}_a^4 + d_1\hat{J}^2(\hat{J}_+^2 - \hat{J}_-^2) + d_2(\hat{J}_+^4 - \hat{J}_-^4), \tag{3}$$

with the step operators $J_+ = J_b + iJ_c$ and $J_- = J_b - iJ_c$.

A. The methyl torsion

In *p*-cresol the internal rotor axis α lies on the principal axis *a* (see Fig. 1 for a sketch). For this case the Hamiltonian for the internal rotation and the coupling of internal rotation to overall rotation is given by[6,32]

$$\hat{H}_{\mathrm{ir}} = F(\hat{j}_\alpha - \rho_a\hat{J}_a)^2 + V(\alpha). \tag{4}$$

The first term describes the kinetic energy, where *F* is the reduced rotational constant for the methyl top and $\rho_g = \lambda_g I_\alpha / I_g$, with I_α the moment of inertia of the top, I_g the moments of inertia of the molecule, and λ_g the direction cosine between the internal rotor axis and the principal axis *g* for $g \in \{a,b\}$. The potential energy for the internal rotation for the methyl group can be approximated as

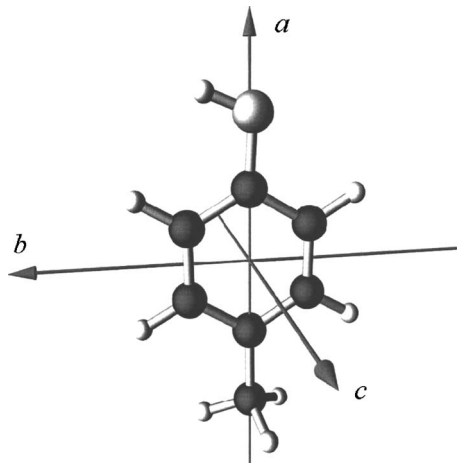


FIG. 1. Sketch of the ground state equilibrium structure of *p*-cresol in its principal axis system.

$$V(\alpha) = \frac{V_3}{2}(1 - \cos 3\alpha) + \frac{V_6}{2}(1 - \cos 6\alpha), \tag{5}$$

where α is the torsional angle of the methyl group relative to the molecular frame.

For molecules with high or medium barrier heights to internal rotations, the above Hamiltonian is sufficient to describe the spectra. For low barriers the spectra can often not be reproduced within the accuracy of the experimental resolution.[12] Results of *ab initio* investigations of such cases show a dependency of the rotational constants on the torsional angle $[A(\alpha) = A_0 + A_1 \cos 3\alpha + A_2 \cos 6\alpha + \cdots]$ (see, e.g., Ref. 33). Hamiltonians taking this dependency into account were suggested in 1970 by Susskind[34] and recently derived from interactions between rotations, internal rotations, and vibrations by Quade.[35] To analyze the methyl torsion we employed such a Hamiltonian,

$$\hat{H}_{it} = A(\alpha)\hat{J}_a^2 + B(\alpha)\hat{J}_b^2 + C(\alpha)\hat{J}_c^2 + F(\alpha)(\hat{j}_\alpha - \hat{J}_a)^2 + V(\alpha), \tag{6}$$

with the Fourier expansion of the rotational constants truncated after $\cos 3\alpha$ and compared the numerical results with an effective and empirical guessed Hamiltonian as implemented in XIAM (Ref. 36)

$$\hat{H}_{\mathrm{eff}} = A_\Gamma\hat{J}_a^2 + B_\Gamma\hat{J}_b^2 + C_\Gamma\hat{J}_c^2 + F(\hat{j}_\alpha - \hat{J}_a)^2 + V(\alpha) \quad \text{with } \Gamma \in \{A,E\}. \tag{7}$$

Both Hamiltonians yielded the same standard deviations when fitting the spectra and gave the same results for the discrete transitions, within one-tenth of the experimental error.

The connection between expressions (6) and (7) can be understood from perturbation theory by expanding the matrix representation of the Hamiltonian in Eq. (6) in a power series. The Hamiltonian matrix can be set up in a basis of products of eigenfunctions of the symmetrical top ($K = -J$ to $+J$) and the free rotor ($m = -\infty$ to $+\infty$) for each total angular momentum *J*. Due to the introduction of cos terms in the rotational constants additional off-diagonal elements in *K* and *m* are produced compared to Eq. (7).

Downloaded 23 Aug 2008 to 134.147.252.238. Redistribution subject to AIP license or copyright; see http://jcp.aip.org/jcp/copyright.jsp

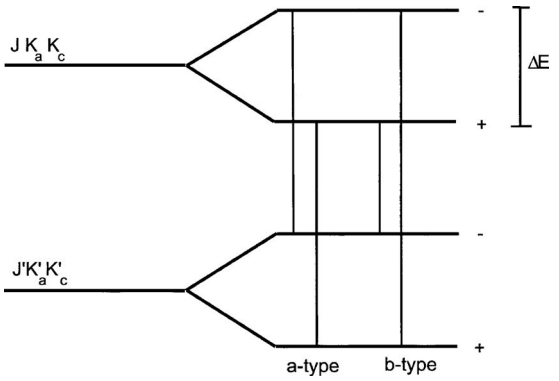


FIG. 2. The splitting of rotational energy levels introduced by the torsion of the hydroxyl group leads to a nonsplit *a*-type transitions and *b*-type transitions split by $2\Delta E$.

$\hat{H}_{rt}$ consists of a diagonal part $\hat{H}_0$ and an off-diagonal part $\hat{H}_3$, which can both be split into rotational (r) and torsional contributions (t):

$$\hat{H}_{rt} = \hat{H}_0 + \hat{H}_3 = \hat{H}_{0r} + \hat{H}_{0t} + \hat{H}_{3r} + \hat{H}_{3t} = \hat{H}_r + \hat{H}_{0t} + \hat{H}_{3t}. \tag{8}$$

A van Vleck transformation factorizes $\hat{H}_r$ into submatrices for each torsional state. The A and E sublevels of the lowest torsional states obtain a different set of effective rotational constants through this transformation. In this sense $\hat{H}_{\text{eff}}$ can be considered as a perturbative expression of $\hat{H}_{rt}$. Effects of centrifugal distortion introduced by the internal rotation are incorporated by the effective expression[36]

$$\hat{H}_{\text{tr-cd}} = \Delta_{Km}[\hat{J}_a^2, \hat{\pi}_\alpha^2]_+ + \delta_m[\hat{J}_b^2 - \hat{J}_c^2, \hat{\pi}_\alpha^2]_+, \tag{9}$$

with $\hat{\pi}_\alpha = \hat{j}_\alpha - \rho_\alpha \hat{J}_a$ and $[x,y]_+$ denoting the anticommutator. Δ_{Km} and δ_m represent the internal-rotation overall-rotation distortion.

B. The hydroxyl torsion

The hydroxyl group is, in principle, an asymmetrical top. The tunneling between the two equal energetic minima leads to a splitting of the rotational energy levels, which can be expressed by a block-diagonal Hamiltonian matrix of the form[19]

$$H_{\text{OH}} = \begin{pmatrix} H_+ & 0 \\ 0 & H_- + \Delta E \end{pmatrix}, \tag{10}$$

where ΔE denotes the energetic splitting of the + and − sublevels.

In the case of *p*-cresol the hydroxyl group rotates around the principal axis a. Due to the small off-axis mass of the hydrogen atom, it is possible to describe the internal motion approximately as a symmetrical top on an asymmetrical frame in a twofold potential similar in structure to the potential in Eq. (5) with

$$V(\beta) = \frac{V_2}{2}(1 - \cos 2\beta) + \frac{V_4}{2}(1 - \cos 4\beta). \tag{11}$$

C. Top-top interactions

The Hamiltonian for the combination of the two internal motions can be written as

$$\hat{H} = \hat{H}_{\text{rot}} + \hat{H}_{\text{cd}} + F_1(\hat{j}_\alpha - \hat{J}_a)^2 + F_2(\hat{j}_\beta - \hat{J}_a)^2 + 2F_{12}(\hat{j}_\alpha - \hat{J}_a)(\hat{j}_\beta - \hat{J}_a) + V(\alpha,\beta), \tag{12}$$

with an additional kinetic constant $F_{12} = I_a/(2I_\alpha I_\beta)$. The potential for the rotation of the two rotors can be expanded as[37]

$$\begin{aligned} V(\alpha,\beta) = {} & \frac{V_6}{2}(1 - \cos 6\alpha) + \frac{V_2}{2}(1 - \cos 2\beta) \\ & + \frac{V_4}{2}(1 - \cos 4\beta) + V_{cc}(1 - \cos 3\alpha \cos \beta) \\ & + V_{c3c}(1 - \cos 3\alpha \cos 3\beta) + V_{ss}(1 \\ & - \sin 3\alpha \sin \beta) + V_{s3s}(1 - \sin 3\alpha \sin 3\beta) \\ & + V_{2c2c}(1 - \cos 6\alpha \cos 2\beta) + \cdots, \end{aligned} \tag{13}$$

where the coupling terms depending on both variables describe the top-top interaction. If the hydroxyl group is in plane ($\beta = 0°$ or 180°) and only the torsion of the methyl group is considered, the coupling terms describe approximately the contribution with threefolded symmetry to the relaxed potential for the methyl torsion in Eq. (5), i.e., $V_{cc} + V_{c3c} \approx V_3/2$.

Furthermore, deformations of the internal rotors during the torsion could be accounted for by including additional Fourier terms in the expansion of the kinetic energy, but the experimental data are not sufficient to analyze this effect.

III. ANALYSIS OF THE MICROWAVE SPECTRA

The microwave spectra for the electronic ground state have been reported in two theses.[38,39] They have been recorded with a Balle and Flygare-type[40] spectrometer, which has been described in Ref. 41. A brief summary of the experimental detail is given in the supplementary material[37] (for further details we refer to Refs. 38 and 39).

All *b*-type transitions of the A species were found to have a splitting of about 175 MHz while the *a*-type transitions are unsplit. This is due to the different selection rules for *a*- and *b*-type transitions, as sketched in Fig. 2. The *a*-type transitions and the arithmetic mean of the *b*-type transitions follow an asymmetric rotor pattern.

For the *b*-type transitions of the E species a splitting of 162 MHz was found. The different splittings of *b*-type transitions for the A and E species lead to the presumption that the top-top interaction perturbs the spectra. In a first step towards assigning the spectra of the E species the arithmetic means of the *b*-type transitions and the *a*-type transitions were included in fits of molecular parameters with the program XIAM (Ref. 36) in order to locate and record all the transitions in the frequency range of the spectrometer. The molecular parameters determined by a least-squares fit of these transitions are presented in Table I. The measured transitions and their observed-to-calculated differences from this fit are given in the supplementary material.[37]

Downloaded 23 Aug 2008 to 134.147.252.238. Redistribution subject to AIP license or copyright; see http://jcp.aip.org/jcp/copyright.jsp

TABLE I. Molecular parameters of *p*-cresol in Watson's *S* reduction.

		A	E
A	(GHz)	5.494 57(2)	5.495 96(2)
B	(GHz)	1.456 963(3)	1.456 85(2)
C	(GHz)	1.160 200(3)	1.160 31(2)
D_J	(kHz)	0.038(1)	
D_{JK}	(kHz)	0.060(7)	
D_K	(kHz)	3.01(9)	
d_1	(kHz)	−0.0107(8)	
d_2	(kHz)	−0.0018(3)	
Δ_{Km}	(MHz)	0.80(3)	
δ_m	(MHz)	−0.059(9)	
V_3	(GHz)	551(1)	
V_3	(cm^{-1})	18.39(3)	
V_6	(GHz)	−220(18)	
V_6	(cm^{-1})	−7.3(6)	
I_α	(amu Å^2)	3.159[a]	
$\angle(\alpha,a)$[b]	(°)	0.0	
$\angle(\alpha,b)$[b]	(°)	90.0	
$\angle(\alpha,c)$[b]	(°)	90.0	
σ[c]	(kHz)	6.7	
N[d]		120	58

[a]Fixed to value given in Ref. 36 because it could not be determined.
[b]Angle between the internal rotor axis and the principle axis, fixed in the fit.
[c]Standard deviation.
[d]Number of transitions.

The torsional splitting of the *A* species was assigned using the Hamiltonian [Eq. (10)] with two separate sets of effective rotational constants for the 0_+ and 0_- sublevels and ΔE as model parameters. No coriolis coupling constants were needed to describe the spectra. Thereafter, the OH torsion was treated as a symmetric rotor with a twofold potential barrier with only one set of effective rotational constants and V_2 as a model parameter in the fitting procedure. Hereby, the same standard deviation of the fits was reached with even less model parameters. The results of the least-squares fits for the parameters of the hydroxyl torsion are given in Tables II and III. Two small programs were written for this comparison using standard matrix diagonalization and least-squares fit routines. Only *b*-type transitions of the *A* species with $J \leqq 3$ were used in these fits to exclude centrifugal distortion effects. The methyl torsion is assumed to be frozen in this consideration. It can be seen that the small mass of the hydrogen in the hydroxyl group leads only to a negligible tilt around the *a* axis of the molecule and that the formalism of internal rotation can very well be applied.

TABLE II. Molecular parameters describing the hydroxyl torsion with a two-state Hamiltonian. The rotational constants are effective ones calculated from the pseudorigid rotor pattern of the *A* species.

		0_+	0_-
A'	(GHz)	5.678 241 8(3)	5.678 206 7(3)
B'	(GHz)	1.456 972 7(2)	1.456 973 1(2)
C'	(GHz)	1.160 189 6(2)	1.160 189 1(2)
ΔE	(GHz)	0.807 773(1)	
σ[a]	(kHz)	7.7	
N[b]		20	

[a]Standard deviation.
[b]Number of transitions.

TABLE III. Molecular parameters describing the hydroxyl torsion as an internal rotation. The rotational constants are effective ones calculated from the pseudorigid rotor pattern of the *A* species.

A''	(GHz)	5.678 224(5)
B''	(GHz)	1.456 974 8(5)
C''	(GHz)	1.160 187 5(5)
V_2	(GHz)	30 945.76(5)
V_2	(cm^{-1})	1032.2(2)
F_0[a]	(GHz)	631.73
σ[b]	(kHz)	7.7
N[c]		20

[a]Fixed to results from the MP2/cc-pVTZ calculation.
[b]Standard deviation.
[c]Number of transitions.

To get an estimate of the ring mediated top-top interaction a program was written to set up the Hamiltonian [Eq. (12)] in the principal axis system and to calculate the energy eigenvalues. The free rotor basis functions were used for each top. For the rotational main quantum number $J=0$ the ΔE value of the *A* and *E* species can be calculated with different model parameters and compared with the observed splittings. Due to the strong correlation of the potential terms, only the leading contribution to the top-top interaction could be determined, which according to the Fourier analysis of the calculated potential should be $V_{cc}(1-\cos 3\alpha \cos \beta)$. Therefore, only V_{cc} was used as model parameter in the fitting procedure; all other molecular parameters were fixed to the values given in Tables I and III. From the fit of the observed splittings only the absolute value of V_{cc} can be determined, but not its sign, i.e., wether the top-top interaction favors the syn- or the antiperiplanar orientation of the two rotors. Due to the limited information and the number of assumptions, the values given in Table IV should be seen as rough estimates.

IV. THEORETICAL INVESTIGATIONS

For the quantum chemical calculations MP2 and the approximate coupled-cluster singles-and-doubles model[28] CC2 have been used for the ground state and the ADC(2) and CC2 for the electronically excited state. These calculations have been carried out with the RICC2 program,[42] which is part of the TURBOMOLE package.[43] For the geometry optimizations recent implementations[44,45] of the analytic gradients for ground and excited states have been employed. The accuracy and the computational performance of the implementation using the resolution-of-the-identity (RI) approximation[46,47] have been demonstrated in Refs. 44 and 48. The correlation-consistent basis sets, cc-pVXZ (X=D,T,Q,5), of Dunning

TABLE IV. The leading potential term of the top-top interaction. No statement on the sign can be made from the experimental results. For the least-squares fits the molecular parameters from Tables I and III were used.

V_{cc}	(GHz)	(−) 200(20)
V_{cc}	(cm^{-1})	(−) 7(1)
ΔE_A[a]	(MHz)	87.6
ΔE_E[a]	(MHz)	81.5

[a]Observed splitting of *b*-type transition for the *A* and *E* species.

Downloaded 23 Aug 2008 to 134.147.252.238. Redistribution subject to AIP license or copyright; see http://jcp.aip.org/jcp/copyright.jsp

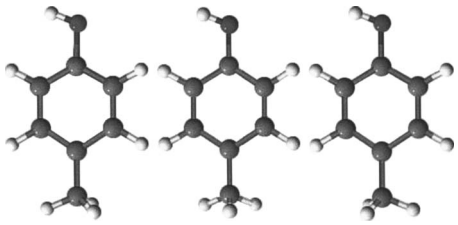


FIG. 3. The characteristic positions of the methyl group with respect to the hydroxyl group are from left to right: eclipsed, perpendicular, and staggered.

and co-workers have been used,[49,50] together with optimized auxiliary basis sets[51,52] for the RI approximation.

The potential energies have been calculated on a 10° grid for the torsional angle (i.e., the dihedral angle of one hydrogen with respect to the benzene ring plane). We varied the torsional angle of the methyl group α from the eclipsed positions to the staggered position, optimizing all other parameters to determine the "relaxed potential" along the minimum energy path. In the eclipsed position of the methyl group one hydrogen lies in the ring plane and is synperiplanar to the hydroxyl group, while in the staggered position it is antiperiplanar to the hydroxyl group. These conformations are sketched together with the intermediate perpendicular conformation in Fig. 3. The parameters V_3 and V_6 of the potential function in Eq. (5) have been determined by a least-squares fit to the points on this grid. The energy in the eclipsed position has been arbitrarily set to zero. Zero point vibrational energy has been neglected in this study because its variation is very small between the different conformations of the methyl group and numerical second derivatives are not accurate enough to improve the potential surface.

The changes in bond lengths and bond angles between geometries obtained in the cc-pVTZ and the cc-pVQZ basis set were found to be very small. Therefore, single point calculations with the cc-pV5Z basis set have been carried out using the cc-pVQZ geometries. To estimate the basis set limit in the ground state, the correlation energy has been extrapolated using the two point formula[53]

TABLE V. Calculated potential parameters for the methyl torsion in the ground state on MP2 and CC2 levels with increasing basis sets. All values are given in GHz.

		MP2	CC2
cc-pVDZ	V_3	588.1	665.4
	V_6	−303.1	−300.9
cc-pVTZ	V_3	510.4	587.3
	V_6	−444.8	−435.0
cc-pVQZ	V_3	474.4	558.4
	V_6	−359.1	−340.5
cc-pVQZ//cc-pV5Z	V_3	475.3	554.6
	V_6	−215.5	−194.0
cc-pVQZ//cc-pV(Q5)Z	V_3	473.8	550.5
	V_6	−60.2	−36.3
Expt.[a]	V_3	551(1)	
	V_6	−220(18)	

[a]This work.

TABLE VI. Calculated potential parameters for the methyl torsion in the first electronically excited state on ADC(2) and CC2 level with increasing basis sets. All values are given in GHz.

		ADC(2)	CC2
cc-pVDZ	V_3	388.8	359.7
	V_6	−779.4	−840.4
cc-pVTZ	V_3	442.8	396.3
	V_6	−1062.5	−1113.0
cc-pVQZ	V_3	441.2	396.7
	V_6	−842.7	−894.1
cc-pVQZ//cc-pV5Z	V_3	414.1	375.7
	V_6	−628.9	−674.2
Expt.[a]	V_3	239.5(1)	
	V_6	−740(1)	

[a]From Ref. 27.

$$E_{XY} = \frac{X^3 E_X - Y^3 E_Y}{X^3 - Y^3}, \tag{14}$$

with $X=Q$, $Y=5$, and has combined the Hartree-Fock (HF) SCF energy from the cc-pV5Z basis.

The results for the internal rotation of the methyl ground are listed in Table V for the ground and in Table VI for the first electronically excited state. The calculations for the internal rotation of the hydroxyl group have been performed in the same manner but using only the cc-pVTZ basis set. The torsional angle β of the hydroxyl group has been varied between the in-plane position, which has the lowest energy, and the perpendicular position. Using the potential function in Eq. (11), the parameters V_2 and V_4 have been determined by a least-squares fit to the calculated points (see Table VII).

The parameters for the top-top interaction potential have been calculated by constraining both torsional angles, α and β, optimizing again all other internal coordinates. To obtain an accurate description of the such defined relaxed potential energy surface, over 100 geometry optimizations have been carried out. Due to this large number, the investigation was only done with CC2 in the cc-pVTZ basis. The calculated energies as a function of the two torsional angles and the Fourier coefficients, which were used to get an accurate description of the two-dimensional surface, are listed in the

TABLE VII. Calculated potential parameters for the hydroxyl torsion in the ground and first electronically excited states using the cc-pVTZ basis set. All values are given in GHz.

		MP2	CC2
	V_2	35 275	39 778
	V_4	−1101	−1413
Expt.[a]	V_2	30 945.76(5)	
		ADC(2)	CC2
	V_2	96 170	96 784
	V_4	−12 202	−12 749
Expt.[b]	V_2	131 759	

[a]This work.
[b]From Ref. 27.

Downloaded 23 Aug 2008 to 134.147.252.238. Redistribution subject to AIP license or copyright; see http://jcp.aip.org/jcp/copyright.jsp

TABLE VIII. Values for the potential terms of the top-top interaction from CC2/cc-pVTZ calculations. All values are given in GHz.

	S_0	S_1
V_{cc}	211	−100
V_{c3c}	86	−39
V_{2c2c}	0	−49

supplementary material.[37] The potential terms for the top-top interaction obtained by a least-squares fit to these results are given in Table VIII.

The sum of V_{cc} and V_{c3c} is approximately $V_3/2$, as calculated with CC2/cc-pVTZ (Tables V and VI). This means that the results for the two-dimensional potentials [Eq. (13)] at $\beta=0$ (OH group in the ring plane) are close to those for the one-dimensional potentials for the methyl group with an optimized orientation of the OH group. Terms proportional to products of sinus functions of the two torsional angles are found to be negligible for the *ab initio* calculated potential energy surfaces.

The calculated rotational constants, determined at the (unconstrained) equilibrium structure of *p*-cresol, are compared with the observed rotational constants in Table IX. (Cartesian coordinates of the structures are listed in the supplementary material.[37]) In the global energy minima of both the ground and the excited state, the OH group lies in the ring plane and the CH_3 group is nearly in the perpendicular position. The calculated structures are equilibrium (r_e) structures, while the experimental results refer to the zeroth vibrational states. Thus, the structures are not exactly comparable, but the effect is very small. The agreement of the rotational constants in Table IX is excellent in both the ground and the excited state.

TABLE IX. Comparison of the rotational constants from calculations and experiments. All values are given in GHz.

	S_0		
	A	*B*	*C*
MP2/cc-pVTZ	5.5219	1.4609	1.1635
MP2/cc-pVQZ	5.5366	1.4654	1.1671
CC2/cc-pVTZ	5.5063	1.4576	1.1608
CC2/cc-pVQZ	5.5210	1.4621	1.1641
Expt.[a]	5.494 57(2)	1.456 963(3)	1.160 200(3)
	S_1		
	A	*B*	*C*
ADC(2)/cc-pVTZ	5.1624	1.4795	1.1587
ADC(2)/cc-pVQZ	5.1765	1.4855	1.1629
CC2/cc-pVTZ	5.1489	1.4744	1.1548
CC2/cc-pVQZ	5.1630	1.4804	1.1590
Expt.[b]	5.155(1)	1.4705(7)	1.1536(4)

[a]This work.
[b]From Ref. 27.

V. DISCUSSION

A. Experimental results

p-cresol is a molecule with very low barrier hindering the internal rotation of the methyl group. The assignment of the rotational spectra of such systems is not straightforward because effects that are negligible for molecules with larger barriers disturb the energy levels here significantly. If higher-order effects, such as those described in Sec. II A, are not taken into account, fitted molecular parameters will not accurately reproduce the recorded spectra and not take full advantage of the assembled data.

For *p*-cresol it was, in particular, found necessary to include the V_6 term of the potential energy function in Eq. (5) because V_3 and V_6 are in the same order of magnitude. For $V_3 \gg V_6$ the numerical correlation between their entries in the Hamiltonian matrix would approach 1 in the torsional ground state. Information about V_6 can then only be obtained from transitions out of higher torsional excited states,[54] which are usually not reachable in very cold molecular beams.

The torsion of the hydroxyl group can be analyzed with about the same accuracy using either a two-state Hamiltonian or the Hamiltonian for a hindered rotation in a potential with two minima. The latter approach has two conceptional advantages. Firstly, the potential barrier, determined from such an analysis, can be compared conveniently with results from *ab initio* calculations (*vide infra*), and, secondly, it facilitates the inclusion top-top interactions in the Hamiltonian. Due to the complicated influence of the top-top interaction on the position of the microwave transitions, only few experimental studies could determine potential parameters for molecules with two interaction tops, although the formalism has been known for a long time.[32] In the present study it has, to our knowledge, been possible for the first time to obtain an estimate for the coupling potential V_{cc} between two tops of different torsional symmetry. The fair agreement with *ab initio* results for this parameter is an indication that the assumptions, which were necessary to derive it, are appropriate.

B. Quantum chemical results

MP2 and CC2 include similar expressions for double excitations in the wave function equations and handle correlation effects through the same order. In CC2, additionally, the single excitations are included. This makes CC2 somewhat more expensive in terms of computational timings than MP2 but allows us to apply linear response theory for calculations on excited states. The differences between MP2 and CC2 results (see Table V) fall within the range of the methodic error at this level. The CC2 values are for *p*-cresol closer to the experimental results than the MP2 values, but this is not valid in general. For *m*-cresol[12] MP2 performed slightly better than CC2. Since both methods are correct through second order in the fluctuation potential, none is superior to the other.[48]

The investigation of basis set convergence is crucial in coupled-cluster theory because the basis set incompleteness error should not be larger than the error of the method for an appropriate discussion of the results. For first-row main group elements double-ζ basis sets cover about 65% of the correlation energy, polarized triple-ζ basis sets cover about

Downloaded 23 Aug 2008 to 134.147.252.238. Redistribution subject to AIP license or copyright; see http://jcp.aip.org/jcp/copyright.jsp

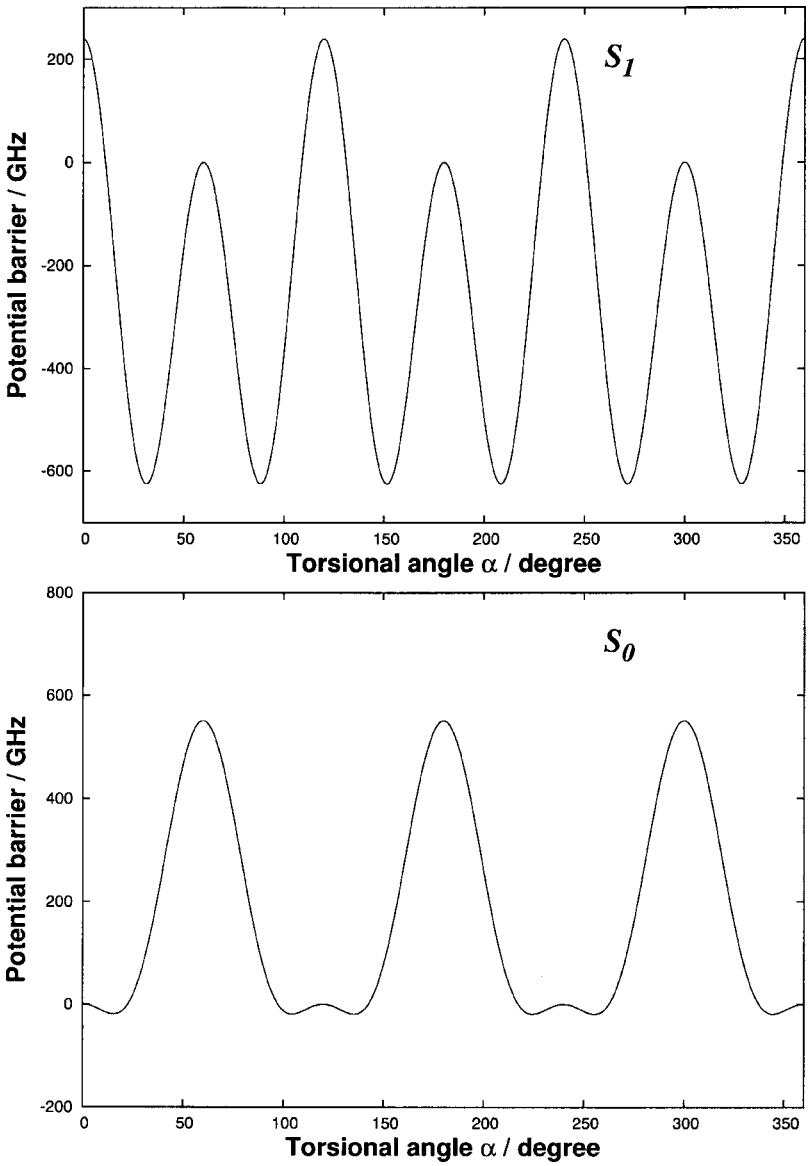


FIG. 4. The potential energy functions $V(\alpha+\Delta\phi)$ in S_1 (upper) and S_0 (lower) plotted with the coefficients from experiments. The functions in S_1 is shifted by a phase factor $\Delta\phi=60°$ ($\Delta\phi=0°$ in S_0) in order to start both plots with the eclipsed structures.

85%, and the quadruple-ζ and the quintuple-ζ basis sets cut the remaining errors further in halfs. The quadruple/quintuple extrapolation should be close to the basis set limit. For MP2 and CC2 the triple-ζ basis set gives a balanced description of the potential energy surface in the ground and in the excited state (Table VI) and was used to study the torsion of the hydroxyl group and the top-top interactions.

In the electronically excited state we used ADC(2) besides CC2. Both methods include electron-electron correlation effects on the excitation energies through second order and lead to excitation energies of the same quality. ADC(2) has no unique defined ground state model, but MP2 is used as a natural choice to assign a ground state energy. This combination leads to a significant reduction of the computational costs compared to the CC2 model. Furthermore, ADC(2) has, in contrast to CC2, a symmetric Jacobian, which leads to additional computational simplifications for the calculation of the excited state gradients. In Table VI it can be seen that the performance of both methods is nearly the same. Thus, MP2 and ADC(2) give for this problem at lower computational costs results of the same quality as CC2. Yet, CC2 has the conceptual advantage of using the same theoretical model in ground and excited states.

In Fig. 4 the potential functions of the methyl torsion in the ground and the excited state are compared. At first sight it can be seen that it is a threefold potential perturbed by a sixfold potential in S_0, while in S_1 it is a sixford potential perturbed by a threefold potential. The orientation of the OH group has a larger influence on the methyl group in S_0 than it has in S_1.

At the Hartree-Fock level the eclipsed structure is the most stable conformation, but the dynamic electron correlation included at the MP2 and CC2 stabilizes the perpendicular structure. This theoretical finding is in agreement with a detailed experimental investigation on toluene by Borst and Pratt,[55] where the perpendicular position was also spotted to be the most stable in S_0 and S_1. An analysis of the Mulliken overlap populations shows that all hydrogens of the methyl group have overlaps with the carbon atoms in the benzene ring in this position, while in the eclipsed and staggered positions the hydrogens in plane have no overlap contributions with the carbon atoms. This suggests that hyperconjugation

Downloaded 23 Aug 2008 to 134.147.252.238. Redistribution subject to AIP license or copyright; see http://jcp.aip.org/jcp/copyright.jsp

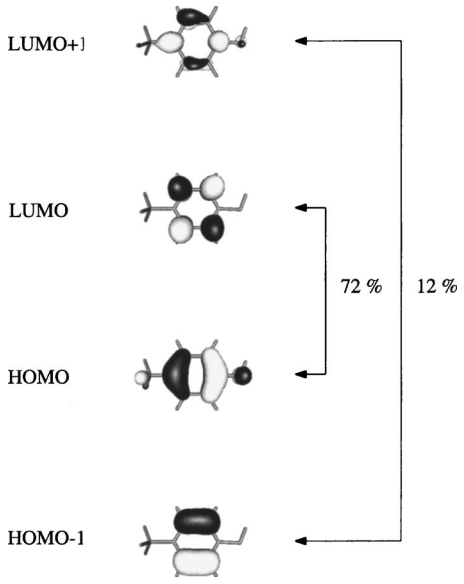


FIG. 5. The most important molecular orbitals (MOs) involved in the S_0-S_1 vertical excitation at ground state equilibrium geometry. The contributions to the excitation energy are given in percent.

is the reason for the stabilization of the perpendicular position. Hyperconjugation is an effect which arises purely from electron correlation. Thus, calculations which did not include dynamic electron correlation[24] or used too small basis sets[25] could not find this minimum.

An asymmetry in the highest occupied molecular orbital (HOMO) leads to a asymmetrical charge distribution, from which the difference between the eclipsed and staggered positions can be explained. In the eclipsed position there is slightly more negative charge at the C_{ring} neighboring the H_{methyl}, which is in plane, compared to the situation in the staggered position. Therefore, the eclipsed position is stabilized by electrostatic attraction. This can already be described qualitatively correct at the HF level. In the excited state the HOMO is depopulated and this difference is leveled out. This can be understood from the visualization of molecular orbitals (MOs) involved in the electronic excitation, as shown in Fig. 5. The largest contributions to the S_0-S_1 excitation are from frontier orbitals—in particular, from delocalized π-bonding MOs into antibonding MOs. This leads to a destabilization of the bonds and a widening of the ring system. Also, the shortening of the C–O and $C-C_{\text{methyl}}$ bonds can be understood. A significant quinoidal distortion cannot be found.

While the height of the potential barrier for the methyl torsion does not change significantly between S_0 and S_1, the hydroxyl torsion is by a factor of about 3 stronger, hindered in the excited state than in the ground state. This is due to a decrease of the electron density in the oxygen lone pair. This decrease is also the reason for an increase in acidity in the excited state, which is typical for phenol derivatives.

VI. SUMMARY AND CONCLUSIONS

We have investigated the internal rotations in *p*-cresol in the ground state S_0 and the first electronically excited state S_1. The combination of two large-amplitude motions as well as the very low barrier of the methyl torsion made it necessary to take higher-order effects into account for the analysis of the microwave spectra. The applied model successfully explains the rotational spectra. As an interesting feature of the spectra, it was found that a difference in the splitting of *b*-type transitions in *A* and *E* symmetries can be utilized to estimate a top-top interaction term, which can rarely be determined in other two-top molecules.

The calculated two-dimensional potential energy surface allows us to get further insight into the intramolecular dynamics. If the two internal motions were gearing or antigearing motions, the top-top potentials should be dominated by contributions which correlate the two angles as, e.g., $\cos(3\alpha\pm\beta)=\cos(3\alpha)\cos(\beta)\mp\sin(3\alpha)\sin(\beta)$. The analysis of the potential energy surface shows that $\sin(3\alpha)\sin(\beta)$ and other coupling terms depending on the sinus of the torsion angles do not contribute to the top-top interaction. The absence of these terms indicates that the two torsions are not gearing or antigearing motions since the top-top interaction does not depend on the relative orientation of the two rotors $(\alpha\pm\beta)$, but only on the orientation of the individual rotors relative to the plane of the benzene ring. Thus, in *p*-cresol one internal motion modulates the potential for the other by inducing slight changes in the structure of the benzene ring, controlled probably by the conjugation of the lone pair of the OH group with the π system and hyperconjugation between the π system and the methyl group, which are effects of the electronic structure. Experimental and theoretical results agree on the finding that these effects are leveled out in the lowest excited singlet state S_1.

The comparison of experimental data with the quantum chemical calculations shows that the correlated second-order methods used here give a very good characterization of the potential energy hypersurfaces. By comparing accurate gas phase measurements with high-level calculations, internal motions can be unraveled and described in detail, not only in the ground state, but also in electronically excited states.

ACKNOWLEDGMENTS

The experiments were performed at the Institut für Physikalische Chemie in Aachen in the group of Wolfgang Stahl, whose support is acknowledged. The authors would like to thank Michael Schmitt for giving them access to his experimental results at an early state of the work. The computational part of this work was supported by the Deutsche Forschungsgemeinschaft through Project No. HA2588.

[1] J. D. Kemp and K. S. Pitzer, J. Chem. Phys. **4**, 749 (1936).
[2] E. B. Wilson, Jr., Adv. Chem. Phys. **2**, 367 (1959).
[3] J. P. Lowe, Science **179**, 527 (1973).
[4] T. K. Brunck and F. Weinhold, J. Am. Chem. Soc. **101**, 1700 (1979).
[5] R. F. W. Bader, J. R. Cheeseman, K. E. Laidig, K. B. Wilberg, and C. Breneman, J. Am. Chem. Soc. **112**, 6530 (1990).
[6] C. C. Lin and J. D. Swalen, Rev. Mod. Phys. **31**, 841 (1959).
[7] W. Gordy and R. L. Cook, *Microwave Molecular Spectra* (Wiley, New York, 1984).
[8] D. W. Pratt, Annu. Rev. Phys. Chem. **49**, 481 (1998).
[9] M. Head-Gordon and J. A. Pople, J. Phys. Chem. **97**, 1147 (1993).
[10] A. Dreuw and M. Head-Gordon, Chem. Rev. (Washington, D.C.) **105**, 4009 (2005).
[11] A. Welzel, A. Hellweg, I. Merke, and W. Stahl, J. Mol. Spectrosc. **215**,

Downloaded 23 Aug 2008 to 134.147.252.238. Redistribution subject to AIP license or copyright; see http://jcp.aip.org/jcp/copyright.jsp

58 (2002).
[12] A. Hellweg, C. Hättig, I. Merke, and W. Stahl, J. Chem. Phys. **124**, 204305 (2006).
[13] C. Coeur-Tourneur, F. Henry, M. A. Janquin, and L. Brutier, Int. J. Chem. Kinet. **38**, 553 (2006).
[14] M. Ketteler, Kidney Int. **69**, 952 (2006).
[15] O. Suriyaphan, M. Drake, X. Q. Chen, and K. R. Cadwallader, J. Agric. Food Chem. **49**, 1382 (2001).
[16] H. D. Rudolph, H. Dreizler, A. Jaeschke, and P. Wendling, Z. Naturforsch. A **22A**, 940 (1967).
[17] H. D. Rudolph and H. Seiler, Z. Naturforsch. A **20A**, 1682 (1965).
[18] G. E. Herberich, Z. Naturforsch. A **22A**, 761 (1967).
[19] C. R. Quade, J. Chem. Phys. **47**, 1073 (1967).
[20] A. Bauder, E. Mathier, R. Meyer, M. Ribeaud, and H. H. Günthard, Mol. Phys. **15**, 597 (1968).
[21] C. R. Quade, J. Chem. Phys. **48**, 5490 (1968).
[22] N. W. Larsen, J. Mol. Struct. **144**, 83 (1986).
[23] S. A. Kudchadker, R. M. Hedges, and B. J. Zwolinski, J. Mol. Struct. **48**, 259 (1978).
[24] H. F. Hameka and J. O. Jensen, J. Mol. Struct.: THEOCHEM **331**, 203 (1995).
[25] P. R. Richardson, M. A. Chapman, D. C. Wilson, S. P. Bates, and A. C. Jones, Phys. Chem. Chem. Phys. **4**, 4910 (2002).
[26] M. Schmitt, Ph.D. thesis, Universität Heidelberg, 1992.
[27] G. Myszkiewicz, W. L. Meerts, C. Ratzer, and M. Schmitt, J. Chem. Phys. **123**, 044304 (2005).
[28] O. Christiansen, H. Koch, and P. Jørgensen, Chem. Phys. Lett. **243**, 409 (1995).
[29] J. Schirmer, Phys. Rev. A **26**, 2395 (1982).
[30] A. B. Trofimov and J. Schirmer, J. Phys. B **28**, 2299 (1995).
[31] J. K. G. Watson, J. Chem. Phys. **45**, 1360 (1966).
[32] H. Dreizler, Fortschr. Chem. Forsch. **10**, 59 (1968).
[33] K.-L. Lu, F. Weinhold, and J. C. Weisshaar, J. Chem. Phys. **102**, 6787 (1995).
[34] J. Susskind, J. Chem. Phys. **53**, 2492 (1970).
[35] C. R. Quade, J. Chem. Phys. **122**, 204306 (2005).
[36] H. Hartwig and D. Dreizler, Z. Naturforsch., A: Phys. Sci. **51**, 923 (1996).
[37] See EPAPS Document No. E-JCPSA6-127-011727 for the microwave frequencies and computational results. This document can be reached through a direct link in the online article's HTML reference section or via the EPAPS homepage (http://www.aip.org/pubservs/epaps.html).
[38] M. Henssen, Diploma thesis, RWTH Aachen, 2000.
[39] A. Hellweg, *Mikrowellenspektroskopische Untersuchungen zur Intramolekularen Dynamik von p-Toluidin, p-Kresol und p-Thiokresol* (Mainz, Aachen, 2003).
[40] T. J. Balle and W. H. Flygare, Rev. Sci. Instrum. **52**, 33 (1981).
[41] J.-U. Grabow, W. Stahl, and H. Dreizler, Rev. Sci. Instrum. **67**, 4072 (1996).
[42] C. Hättig and F. Weigend, J. Chem. Phys. **113**, 5154 (2000).
[43] R. Ahlrichs, M. Bär, M. Häser, H. Horn, and C. Kömel, Chem. Phys. Lett. **162**, 164 (1989).
[44] C. Hättig, J. Chem. Phys. **118**, 7751 (2003).
[45] C. Hättig and A. Köhn, J. Chem. Phys. **117**, 6939 (2002).
[46] O. Vahtras, J. E. Almlöf, and M. W. Feyereisen, Chem. Phys. Lett. **213**, 514 (1993).
[47] M. W. Feyereisen, G. Fitzgerald, and A. Komornicki, Chem. Phys. Lett. **208**, 359 (1993).
[48] C. Hättig, Adv. Quantum Chem. **50**, 37 (2005).
[49] T. H. Dunning, J. Chem. Phys. **90**, 1007 (1989).
[50] R. A. Kendall, T. H. Dunning, and R. J. Harrison, J. Chem. Phys. **96**, 6796 (1992).
[51] F. Weigend, A. Köhn, and C. Hättig, J. Chem. Phys. **116**, 3175 (2002).
[52] C. Hättig, Phys. Chem. Chem. Phys. **7**, 59 (2005).
[53] A. Halkier, W. Klopper, H. Koch, and J. Noga, J. Chem. Phys. **106**, 9639 (1997).
[54] H. D. Rudolph and A. Trinkaus, Z. Naturforsch. A **23A**, 68 (1968).
[55] D. R. Borst and D. W. Pratt, J. Chem. Phys. **113**, 3658 (2000).

Downloaded 23 Aug 2008 to 134.147.252.238. Redistribution subject to AIP license or copyright; see http://jcp.aip.org/jcp/copyright.jsp